Analysis of Plasma Extraction Transit Time Oscillations in Bipolar Power Devices

Ralf Siemieniec*, Paul Mourick**, Josef Lutz***, Mario Netzel*

* Technical University of Ilmenau, PO BOX 100565, D-98684 Ilmenau
** Consultant Engineer, D-69427 Oberscheidental,
*** Technical University of Chemnitz, D-09107 Chemnitz

GERMANY

Abstract

The occurrence of high-frequency pett oscillations is related to the transit-time of the carrier transport through the already formed space-charge region at the end of the turn-off process of bipolar power devices. These oscillations are found only in case of a matching external LC circuit which acts as a resonance circuit. It is shown that the occurrence of this type of oscillations depends on a wide range of parameters. 3D EMC simulation is used for the estimation of resonance points of the complete power module.

Introduction

Pett (plasma extraction transit time) oscillations are high-frequency oscillations which may occur during the turn-off of bipolar power devices. This phenomenon is a recently discovered effect (1). Pett oscillations were first found in power modules with paralleled IGBT chips (1), but they also occur in modules with paralleled freewheeling diodes (FWD) or even in case of single IGBT chips (2). Recent works show that these oscillations should be avoided due to their adverse influence regarding EMC issues (3).

Experimental Setup

Fig. 1 shows layout and internal circuit of an experimental power module GAR provided by SEMIKRON. The ratings of this module are 1200V and 600A. In this power module, two FWDs as well as two IGBTs are either paralleled in one group at one DCB (direct copper bonding) substrate, while again two groups are paralleled in the module to gain the desired current capability.
Measurements are done using a conventional double-pulse method. For the characterization of the oscillation effect, reverse voltage, forward current and temperature can be chosen freely in a wide range.

EMC and Device Simulation System

The analysis of the EMC properties of the power module was done using the 3D EMC Simulator FLO/EMC (4). The system solves the complete Maxwell equations and offers the possibility to apply an excitation at several ports inside the model. For the characterization of the power modules, the excitation in form of a delta pulse was applied along one freewheeling diode. This is done to calculate the scattering parameters, namely the input impedance (4).
There is no possibility to include real semiconductors into FLO/EMC. Therefore, a simplified model is used which reproduces the correct junction capacitance or on-state resistance of the devices (IGBT and FWD).
For device simulation, the 1D system ADIOS is used (5). ADIOS solves the common semiconductor equations and also considers recombination centers which arise from the use of carrier lifetime control techniques. In case of the investigations done in this work, this becomes important since the FWDs of the power module GAR are CAL diodes (Controlled Axial Lifetime). The properties of the recombination centers were reliable determined in previous work (6,7).

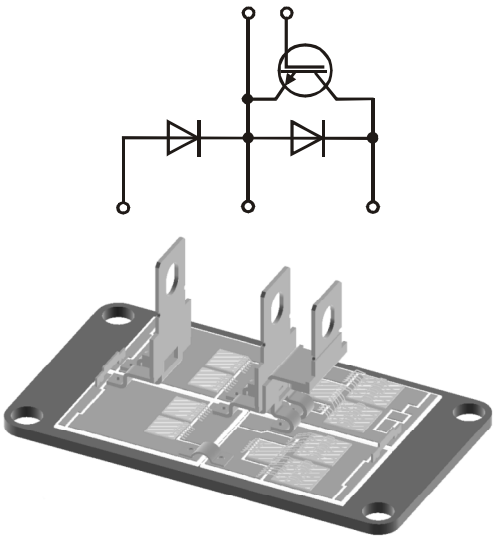

Fig. 1: Internal circuit and layout of the investigated 1200V/600A power module GAR

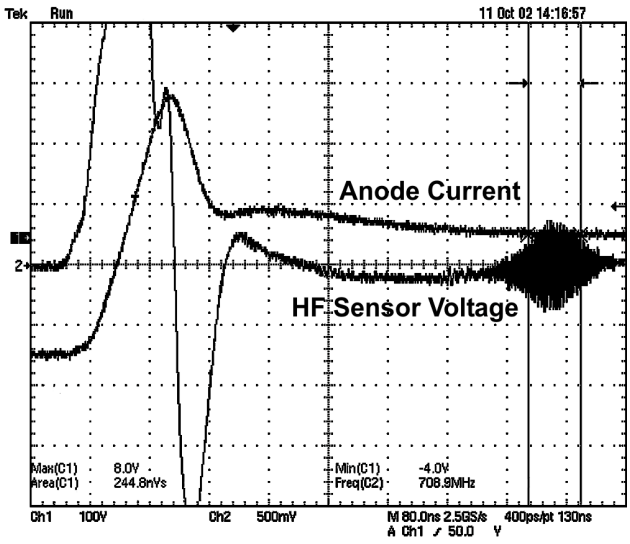

Fig. 2: Measurement of a pett oscillation in power module GAR

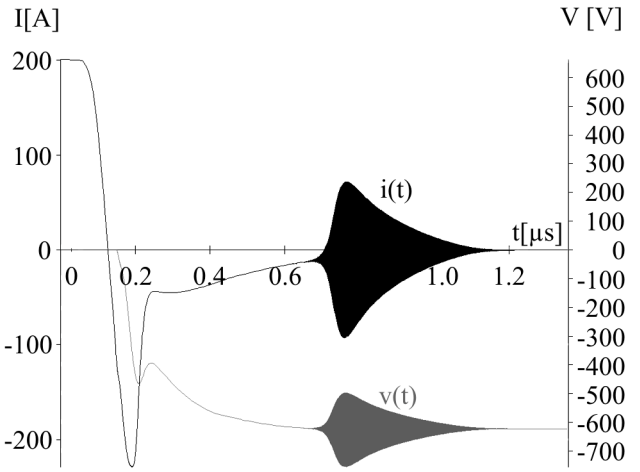

Fig. 3: Pett oscillation as result of device simulation

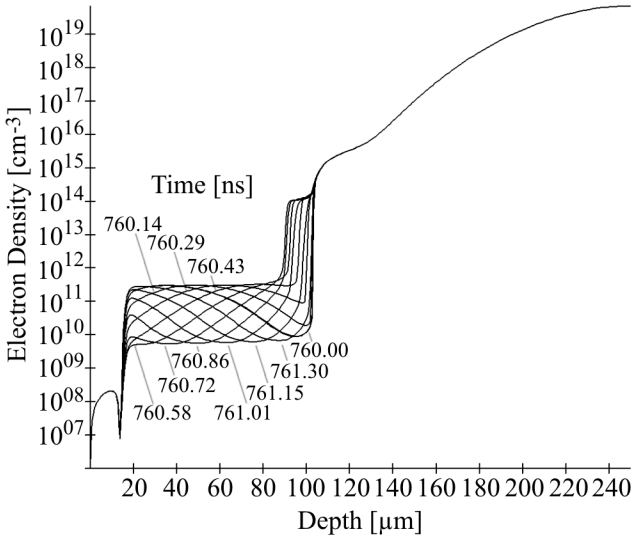

Fig. 5: Electron density along vertical axis at different points in time

Investigation of Pett Oscillation

A. The Effect

Fig. 2 shows the measurement of a pett oscillation which occurs during the turn-off of the power module GAR. Since the oscillation can not be measured directly, an antenna was used to detect the electromagnetic field generated by the oscillations. It is also possible to find this effect in device simulation. As an example, fig. 3 shows the simulation of the turn-off of a single FWD, where pett oscillations are found.

The mechanism of the pett oscillation is related to the mechanism of the baritt diode (8). In difference to the baritt effect, the carrier injection into the space charge region is caused by the stored excess carriers in the remaining plasma in the device during the turn-off process as schematically shown in fig. 4. The holes, flowing with the drift velocity v_d and having the density,

$$p = \frac{j}{q \cdot v_d}$$

will increase the effective doping to,

$$N_{eff}=N_D+p$$

Therefore, the gradient of the electrical field dE/dw is changed. Due to the discontinuous flow of the holes in form of packets, the dE/dw is increased in the location of the packet and decreased in the remaining part of the middle zone as to be seen in fig. 4.

This results in a small negative voltage for the transition of a carrier packet. Oscillations occur if this negative differential resistance is larger than all other positive resistances in the complete circuit. The oscillation frequency for the transit-time effect is given by,

$$f_T = \frac{v_d}{w_{sc}}$$

where w_{sc} is the space charge region width w_{sc} of the semiconductor device and v_d the drift velocity of the carriers. Oscillation will only occur if there is a resonance circuit

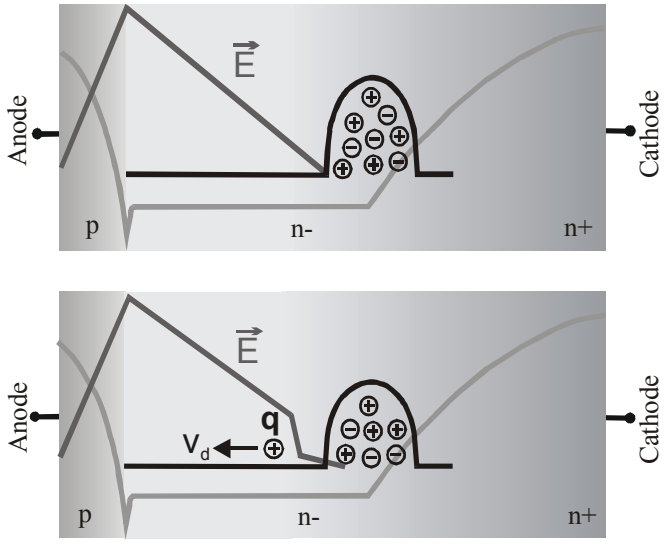

Fig. 4: Origin of pett oscillation due to hole carrier extraction out of a region with high carrier density

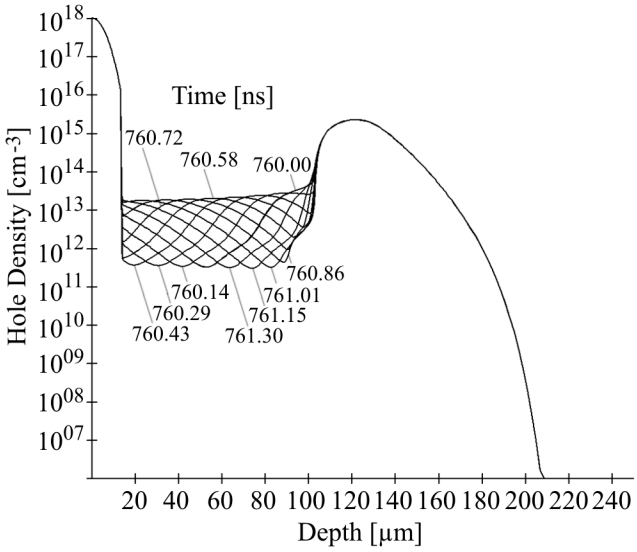

Fig. 6: Hole density along vertical axis at different points in time

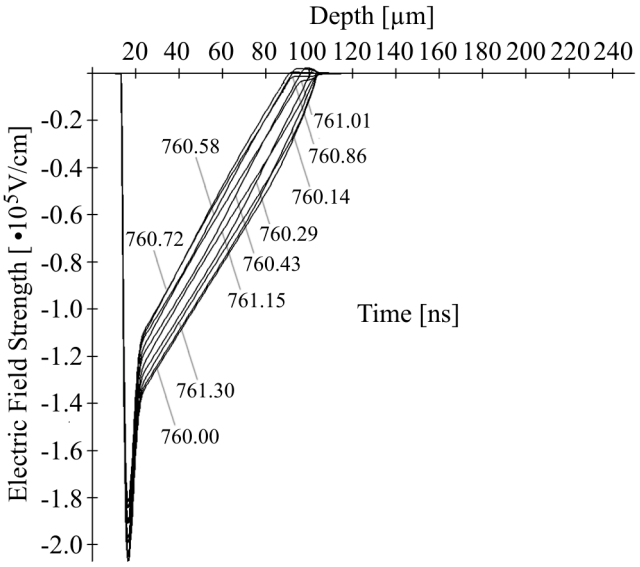

Fig. 7: Electrical field along vertical axis at different points in time

formed by the junction capacitance and the inductance of the bond wires, whose resonance frequency has to be in the order of f_T. This means, an external inductance is necessary and therefore the construction of the power module itself has influence on the appearance of these oscillations.

In the simulation in fig. 5, the electron density is shown along the vertical axis for several points in time. From fig. 5, the cycling of carrier packets is clearly indicated. In fig. 6, the hole densities for different points in time are shown. The hole concentrations are reasonably larger compared to the electron concentrations which gives evidence to the hole extraction from the remaining excess carriers stored at the nn^+-junction of the device. Nevertheless even the number of the travelling holes is rather low in this process, which gives an explanation of the small amplitude of this oscillation.

The simulation shown in fig. 7 depicts the electric field distribution in the device. Here, the change of the gradient of the electric field at different points in time is observed. Again, this change is relatively small due to the low number of travelling carriers.

B. Pett Oscillation Dependencies

The occurrence of pett oscillations depends on a wide number of parameters.

The carrier drift velocity v_d is sensitive to the temperature and the electric field strength E as well. The effective width of the space-charge region w_{sc} mainly depends on the applied voltage. The number of the remaining stored excess carriers depends on the forward current density while the carrier removal process is strongly influenced by the current change in time di/dt which again depends on a number of parameters (gate resistor applied to IGBT, stray inductances etc.).

The resonance frequency of the parasitic LC circuit also depends on a number of parameters. The inductance arising from the bond wires depends on length, diameter, material and number of the bond wires. The capacitance of the power device is governed by the active area and the width of the space-charge region with the already addressed dependencies. Furthermore, the inductive and capacitive parasitics of the power module itself are from importance.

Due to the high number of parameters, it is difficult to predict whether pett oscillations will occur or not. In fig. 8 and in fig. 9, the measured HF sensor voltage is shown in dependence on reverse voltage V_R, forward current I_F, temperature T. The di/dt is controlled by the gate resistor applied to the IGBT, therefore the influence of this parameter is apparently shown as well.

Obviously, the pett oscillation only occurs in a certain parameter range. Nevertheless, within this range the dependencies are rather complex.

C. Avoidance of Pett Oscillations

In general, the oscillation is avoided if there is no LC circuit with a resonance frequency in the range of the transit time. As shown before, the transit time itself depends on a number of parameters and is therefore depending on the bias point of the device. Especially in modern power modules with low parasitics both resonance frequency of the LC circuit and transit frequency of the device are likely to match at certain

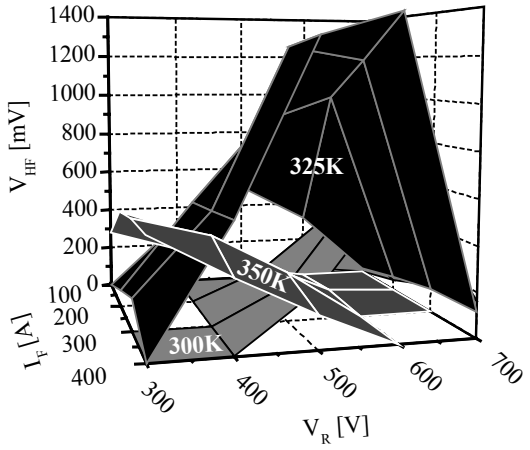

Fig. 8: Measured HF sensor voltage in dependence of reverse voltage, forward current and temperature for R_G=5Ω

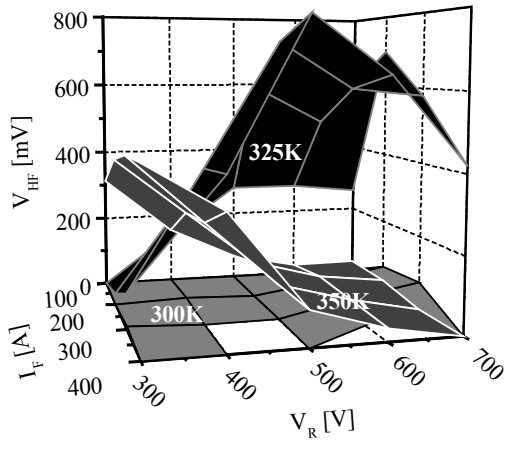

Fig. 9: Measured HF sensor voltage in dependence of reverse voltage, forward current and temperature for R_G=15Ω

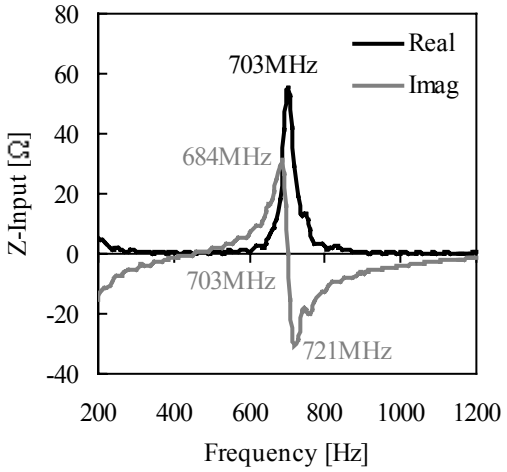

Fig. 10: Impedance of module GAR as seen from FWD

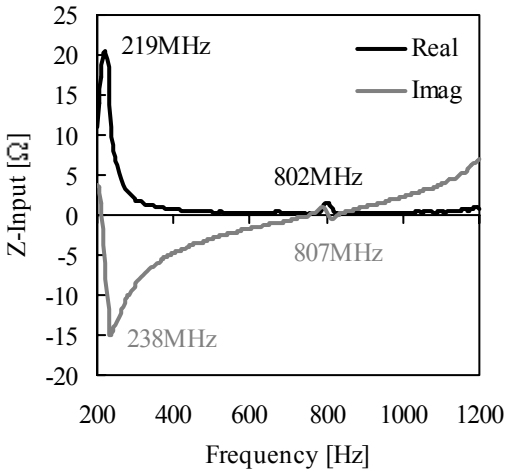

Fig. 12: Impedance of the module with additional bond wires shorting the anode contacts of the FWDs

operating points of the power module.

To find resonance points of the power module layout, the 3D EMC Simulation System FLO/EMC is used (4). Figure 10 shows the calculated impedance (real and imaginery part) of the module GAR as seen by the FWD. It clearly shows a resonance point at 700MHz which is in the range of the transit frequency of the FWD and therefore explains the occurrence of the pett oscillation in this module.

A chance to avoid this oscillations is given by the detuning of the LC circuit. An obvious possibility is to minimize the bond wire inductance by applying additional shorts for the anode contacts as shown in fig. 11. Due to the reduced inductance, the resonance point of the module is expected to move to a higher frequency. Fig. 12 shows the calculated impedance of the power module with these additional bond wires. The resonance point at 700MHz has vanished, no oscillation will occur which is in accordance with comparable results published elsewhere (9).

Conclusion

High-frequency transit-time oscillations in bipolar power semiconductor devices may occur during the tail current phase of the turn-off process. The oscillations investigated in this work are caused by carrier packets extracted from the remaining excess carrier region, which are transported through the already-formed space-charge region and result in the oscillations due to interaction with parasitic LC circuits. Resonance frequency of the power module and transit-time of the carriers are necessary to match.

The oscillations may result in an exceeding of electromagnetic emission limits as defined in several standards and therefore should be avoided.

The mechanism, which leads to these oscillations, is related to the pett (plasma extraction transit-time) effect. In this work, an explanation of the mechanism is given and supported by appropriate device simulations. The complex dependencies of influencing parameters are discussed. Although, due to the large number of dependencies, it is difficult to find a strategy which reliably prevents the occurrence of the pett oscillations, possibilities for the avoidance of this effect are discussed.

The use of a 3D EMC simulation tool for the analysis of the power module itself gives an opportunity to find the resonance frequency and, if necessary, to introduce changes to the module layout. It is shown, that the use of such a tool is of advantage for the prevention of this type of oscillations.

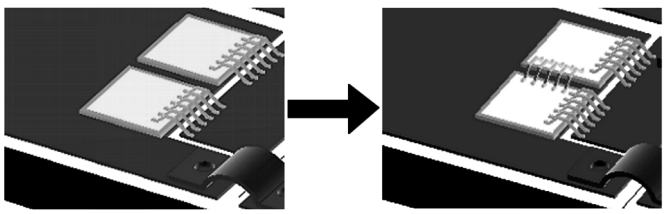

Fig. 11: Power module without and with additional bond wires shorting the anode contacts of the FWDs in one group

References

(1) B.Gutsmann, P.Mourick and D.Silber. Plasma Extraction Transit Time Oscillations in Bipolar Power Devices. *Solid-State Electronics*, 46 (1), 2002, pp. 133-138

(2) P.Mourick, B.Gutsmann and D.Silber. Ultra High Frequency Oscillations in the Reverse Recovery Current of Fast Diodes. In *Proceedings ISPSD,* Santa Fe 2002, pp. 205-208

(3) R.Siemieniec, J.Lutz, P.Mourick and M.Netzel. Transit Time Oscillations as a Source of EMC Problems in Bipolar Power Devices. In *Proceedings EPE*, Toulouse, 2003

(4) Flomerics Limited. *FLO/EMC Reference Manual Release 1.2*. Surrey, UK, 2003

(5) P.Mourick. *ADIOS-Manual*, Nuernberg, 1988

(6) R.Siemieniec, W.Südkamp and J.Lutz, Determination of Parameters of Radiation Induced Traps in Silicon, Solid-State Electronics, 46(6), 2002, pp. 891-901

(7) R.Siemieniec, W.Südkamp and J.Lutz, Applying Device Simulation for Lifetime-Controlled Devices", *Proc. ICCDCS,* Aruba 2002

(8) T.G.van de Roer. *D.C. and small-signal A.C. properties of silicon BARITTT diodes*. Ph.D. Thesis, University of Eindhoven, 1977

(9) W.Zimmermann and K.H.Sommer, *Patent DE 195490011C2*, 1995